Mechanical Engineering – Scientific Journal, Vol. **43,** No. 1, pp. 39–47 (2025)
Number of article: 692
Received: April 17, 2025
Accepted: May 12, 2025
In print: ISSN 1857–5293
On line: ISSN 1857–9191
UDC: 552.581.08-049.8:62/63(497.722)
https://doi.org/10.55302/MESJ2543139k

Original scientific paper

SPECIFIC APPLICATIONS OF DIATOMACEOUS EARTH FROM SLAVIŠKO POLE, REPUBLIC OF NORTH MACEDONIA

Tajana Kostadinova, Andrijana Čankulovska Tenovska, Katerina Atkovska, Gordana Ruseska, Boško Boškovski, Slobodan Bogoevski

Faculty of Technology and Metallurgy, University "Ss Cyril and Methodius" in Skopje, Rugjer Bošković 16, 1000 Skopje, Republic of North Macedonia
tajana@tmf.ukim.edu.mk

A b s t r a c t: Diatomaceous earth from Slaviško Pole, based on the results of mineralogical-petrographic and physico-chemical analyses, exhibits specific characteristics that could be utilized to meet particular industrial, construction, and agricultural requirements. As a raw material predominantly composed of feldspars, K-feldspar of the microcline type, as well as Na-Ca plagioclases of albite-oligoclase type, several species of diatoms, and minor quantities of quartz, iron-bearing minerals, and other trace elements embedded within sedimentary layers, it demonstrates properties that align well with certain application demands. The material has been found to possess exceptionally favorable thermal insulation characteristics in compact segments, making it highly suitable for the construction industry, along with the potential for straightforward mechanical processing. Further investigations into its chemical and mineralogical composition, primary particle size distribution, and mechanical transformation potential have revealed parameters that strongly indicate possible applications in agriculture, including ecological pest control against insects and nematodes, soil conditioning and pH regulation, and passive soil decontamination. Additionally, its applicability in filtration processes for potable and waste water, as well as other fluids, has been identified.

Key words: diatomaceous earth; Slaviško Pole; thermal insulation properties; ecological pest control

МОЖНОСТИ ЗА СПЕЦИФИЧНА ПРИМЕНА НА ДИЈАТОМЕЈСКАТА ЗЕМЈА ОД СЛАВИШКО ПОЛЕ, РЕПУБЛИКА СЕВЕРНА МАКЕДОНИЈА

А п с т р а к т: Дијатомејската земја од Славишко Поле, според резултатите од минералошко-петрографските и физичко-хемиските испитувања, покажува некои специфични карактеристики кои би можеле да се искористат за исполнување конкретни специфични барања во индустријата, градежништвото и земјоделието. Како суровина која доминантно содржи фелдспати, К-фелдспат од типот микроклин, како и Na-Ca плагиокласи на албит-олигоклас, неколку видови дијатомеи, како и минорни количини кварц, железоносни минерали и други микроелементи, сите вклопени во седиментни слоеви, дијатомејската земја покажува особини кои целосно одговараат на некои барања од апликативната лепеза. Утврдени се исклучително позитивни термоизолациони карактеристики на компактни сегменти од суровината, пожелни за градежната индустрија, како и можноста за едноставно механичко конфекционирање. Од другите испитувања на хемискиот и минералошкиот состав, димензиите на примарните честички и можностите за механичка трансформација, утврдени се параметри кои несомнено упатуваат на можна примена на матeријалот во областите на земјоделието (како еколошка заштита на растенијата од инсекти и нематоди, подобрувач на почвата и регулатор на pH, пасивна деконтаминација на почва), а секако и за примена во процесите на филтрација на вода за пиење и отпадна вода, како и други флуиди.

Клучни зборови: дијатомејска земја; Славишко Поле; термоизолациони карактеристики; еколошка заштита од инсекти

1. INTRODUCTION

Diatomaceous earth (DE) is a naturally occurring complex sediment composed of the fossilized remains of diatoms, a class of unicellular algae characterized by intricate silica-based exoskeletons, commonly known as frustules [1–3]. It has unique physicochemical properties, including exceptionally high porosity, low bulk density, and a high specific surface area. Diatomaceous earth exhibits remarkable utility across diverse industrial applications [4–8]. The majority of research on DE focuses on the analysis of its individual components, including its diverse exoskeletal morphologies and its high silica content. The morphological diversity observed among diatoms suggests the potential for multifunctionality, particularly in interactions with a broad spectrum of pathogens. Notably, detailed structural examinations of these frustules provide valuable insights in fields such as biomedical engineering, water purification, and agricultural enhancements, reinforcing the long-held principle that form is inherently dictated by function [9–14]. In 2023, the United States remained the predominant global producer of diatomaceous earth, contributing an estimated 32% of total worldwide output. Denmark followed with a 17% share, while China, Turkey, and Argentina, along with Mexico and Peru, accounted for approximately 10%, 8%, and 4% each, respectively. Furthermore, DE extraction occurred on a smaller scale in 19 additional countries [15]. Among these, North Macedonia possesses substantial DE reserves. The economic viability of DE sourced from North Macedonia is primarily attributed to its fine microstructure and, more significantly, its high content of non-crystalline (amorphous) silica [16–19]. This structural characteristic enhances the material's reactivity, making it particularly advantageous for various applications. The objective of this research is to systematically analyze key fundamental and main characteristics of diatomaceous earth, with the aim of facilitating its optimized utilization in specialized and application-specific contexts.

2. MATERIALS AND METHODS

In the geographical map and satellite image (Figures 1 and 2), the location of Slaviško Pole and the broader area from which diatomaceous earth samples were collected are marked. Slaviško Pole is situated within the contact zone between the Kratovo-Zletovo region and the Serbo-Macedonian Massif. The sampling points are predominantly located along the edges of the former Pliocene lake, where the concentration of diatoms in the overall mass is lower compared to the lower-lying areas of the present-day basin.

The samples collected for analysis are shown in Figure 3 and originate from multiple locations within the site.

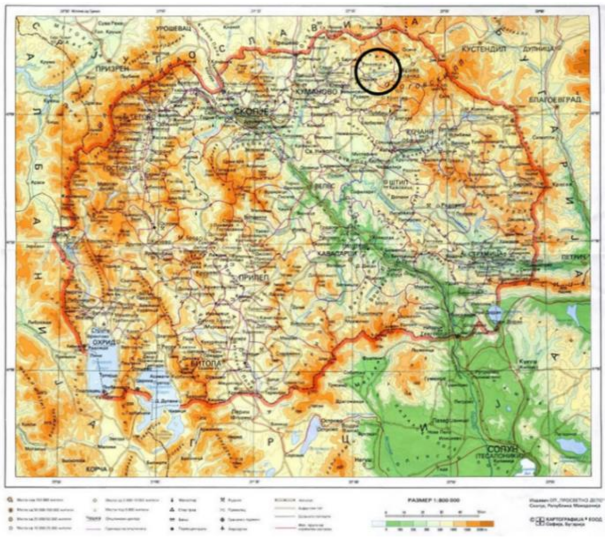

Fig. 1. Geographical location of Slaviško Pole

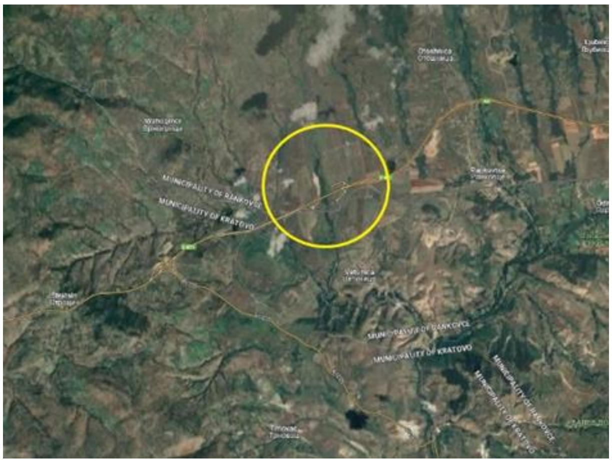

Fig. 2. Satellite image of Slaviško Pole

Fig. 3. Samples of diatomaceous earth from the corresponding sampling points

According to previous studies, X-ray diffraction analysis and transmission optical microscopy reveal the following mineralogical characteristics of this material: a dominant content of fine-grained feldspars (K-feldspar of the microcline type, as well as Na-Ca plagioclases of albite-oligoclase), a significant percentage of amorphous or cryptocrystalline mass, and several species of diatoms [20].

The diatoms, as a component of this material, were identified using transmission optical microscopy (SM-POL type, Letz-Wetzlar, Germany). The chemical composition was determined through silicate chemical analysis with alkaline melting of each fraction, with the fractions obtained via wet sieve analysis following a grinding process (without the presence of porcelain balls) in a porcelain mill for one hour. The presence of trace elements was determined using ICP-MS (Model 7850, Agilent Technologies). Physico-chemical examinations were conducted with standard laboratory equipment, determining specific mass, bulk density, water absorption, open, closed, and total porosity, and compressive strength in both raw and annealed states (ZRMK Ljubljana HPM 400). To determine the size and morphology of the primary grains, SEM analysis (JEOL JSM 35 CF) with an X-ray analyzer (TRACOR NORTHERN TN – 2000) was applied. The characteristic thermal insulation capacity was defined through a custom-designed laboratory test.

3. RESULTS AND DISCUSSION

The granulometric analysis was conducted using a set of sieves with perforation size of 0.1 mm, 0.071 mm, 0.045 mm, and 0.032 mm, following the grinding process in a porcelain mill (without the presence of porcelain balls) for one hour. The obtained results are presented in the histogram shown in Figure 4.

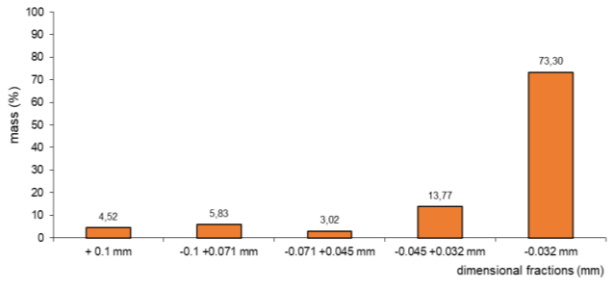

Fig. 4. Histogram of mass content of various dimensional grain fractions after 1 hour milling

Silicate chemical analysis with alkaline melting was performed on each of the dimensional fractions to determine the distribution variations of each component. The results are presented in Table 1.

T a b l e 1

Chemical composition of various dimensional grain fractions (mass %)

	+0.1 mm	–0.1 +0.071 mm	–0.075 +0.045 mm	–0.045 +0.032 mm	–0.032 mm
SiO_2	62.96	60.80	60.96	61.90	64.84
Fe_2O_3	15.96	16.06	15.95	16.16	9.22
Al_2O_3	2.88	2.95	2.90	2.85	6.01
CaO	6.10	7.40	7.40	6.90	3.80
MgO	1.97	2.75	2.70	2.55	1.78
Na_2O	2.61	2.72	2.51	2.72	1.80
K_2O	3.73	4.24	4.24	3.73	1.94
SO_3	tr.	tr.	tr.	tr.	tr.
l.w.	2.92	2.16	2.36	2.33	9.65
Σ	99.13	99.08	99.02	99.14	99.04

From the chemical analysis, it can be concluded that in the finest fraction, the content of alkaline oxides, which are indicators of the presence of feldspars, drastically decreases. Another characteristic of the finest fraction is the highest content of SiO_2 and Fe_2O_3, while, conversely, there is a drastically lower concentration of Al_2O_3. The highest value for weigh loss of ignition at 600°C predominantly originates from the content of organic matter, as shown in Table 2, where the finest fraction contains the dominant content of organic matter in the total mass of the material. The content of trace elements is presented in Table 3.

Table 2

Total content of organic matter (mass %)

Dimensional fraction (mm)	Organic matter content, 600°C (mass %)
+ 0.1	1.72
–0.1 +0.071	0.97
–0.071 +0.045	0.77
–0.045 +0.032	1.12
–0.032	7.34

Table 3

ICP-MS analysis, content of trace elements (ppm)

Element	(ppm)
Ag	<1
Al	39679.60
As	7.10
B	23.86
Ba	337
Ca	15053.90
Cd	<1
Co	<1
Cr	8.95
Cu	25.09
Fe	30398.40
K	12158.90
Li	4.70
Mg	1948.56
Mn	2
Mo	<1
Na	0
Ni	3.82
P	2
Pb	33.93
Sr	0
V	49.80
Zn	79.58

The basic mass of the material is predominantly cryptocrystalline, with quartz and feldspar grains occasionally found in the size range of 0.005–0.01 mm and 0.05–0.1 mm (Figure 5). The feldspar mass is represented by polysynthetic lamellae of plagioclases of the albite-oligoclase type (Figure 6). Within the basic mass, diatom skeletons were also found, exhibiting an elongated shape with longitudinally connected segments measuring approximately 100 µm (Figure 7). Another type of diatom is shown in Figure 8. These skeletons are symmetrically separated longitudinally at the center and represent silicate spicules of the spongolite type. The identification of microfossils in this sediment was carried out through comparative analysis of identical species, which are well-known according to the literature data [21], and *Melosira undulata* [22].

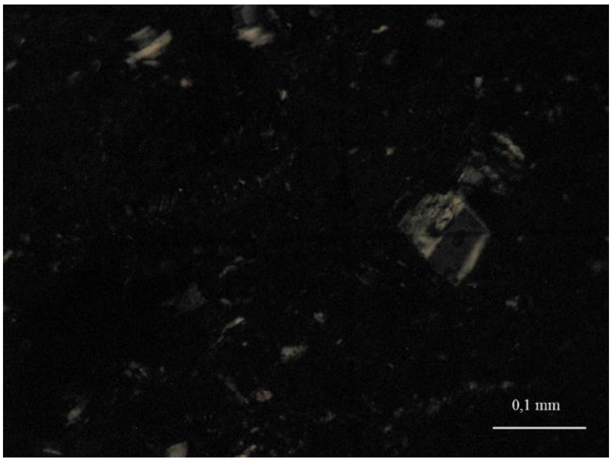

Fig. 5. Photograph of transmissional optical microscopy. Minor crystalline phase in the base mass (N+)

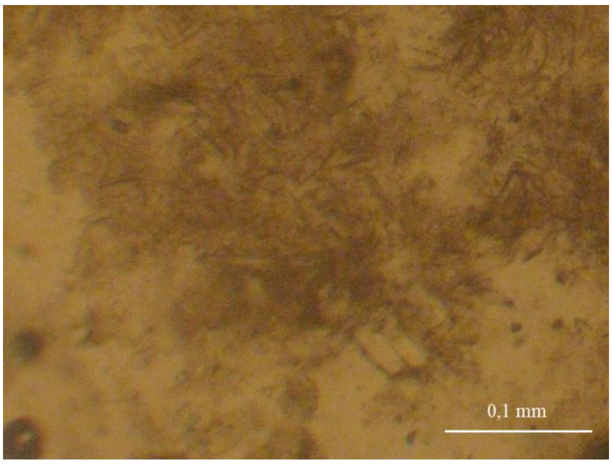

Fig. 6. Photograph of transmissional optical microscopy. Polysynthetic lamellae

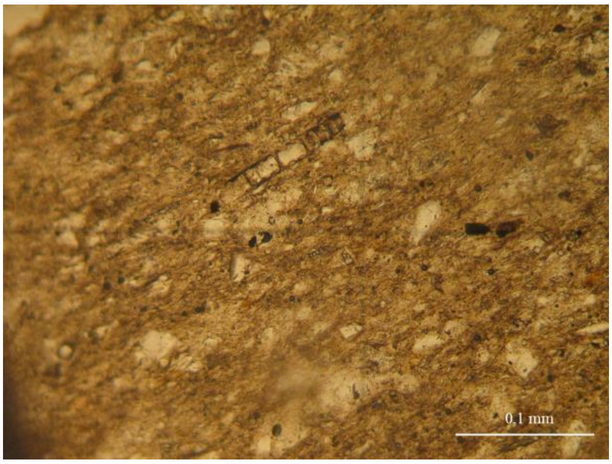

Fig. 7. Photograph of transmissional optical microscopy. Typical longitudinal section of diatoms (*Melosira undulata*) incorporated into basic fine-grained cryptocrystalline amorphous opal mass, in which round grains of feldspar and quartz coexist

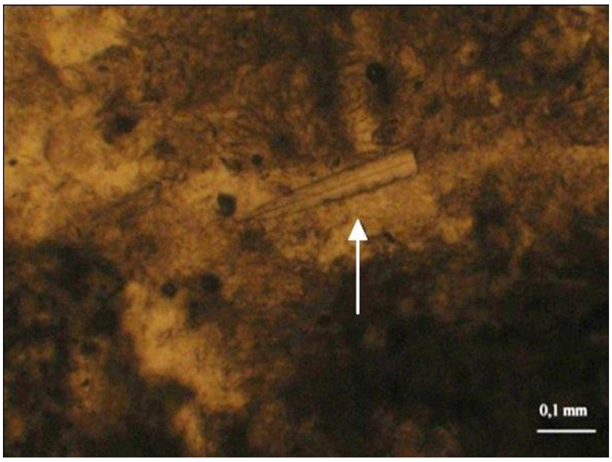

Fig. 8. Photograph of transmissional optical microscopy. *Spongolite spicule* incorporated into cryptocrystalline amorphous opal mass (N+)

Further examinations were conducted to assess certain physico-chemical characteristics, which were divided into several segments. The following physico-mechanical and physico-chemical analysis were performed on the compact sedimentary material of diatomaceous earth: specific mass, bulk density, water absorption, open, closed, and total porosity, and compressive strength. These analyses were carried out on the material in its raw state, treated at 600°C for 2 hours and treated at 800°C for 2 hours. The results of these tests are presented in Table 4.

Table 4

Physical characteristics of the raw material

Physico-мechanical characteristics (properties)		Raw material	Treated at 600°C, 2h	Treated at 800°C, 2h
Specific mass (g/cm³)		2.511	2.533	2.558
Bulk density (g/cm³)		0.95	0.92	0.94
Water absorption (%)		61.46	62.99	62.72
Porosity (%)	Open	58.99	59.81	58.95
	Closed	2.82	2.69	4.30
	Total	61.81	62.50	63.25
Compressive strength (MPa)		7.22/7.30*	17.10	7.25

From the presented results for compressive strength, it can be concluded that the material retains its basic mechanical characteristics in all orientations, both in its original state and after being thermally treated at 600°C and 800°C. This data is significant for the application of diatomaceous earth in compact elements for construction, where it is required that the material, when processed to appropriate dimensions, remains self-supporting.

From the analysis conducted using SEM and EDS, as shown in Figure 9 and Table 5, the dimensions of the primary grains and their aggregates at multiple levels can be clearly observed. The composition is typical of the base mass, confirmed by the other methods.

The material's ability to function as a thermal insulator in its compact form was experimentally demonstrated as follows: a piece of the material, approximately 4 cm thick, was partially perforated from the backside at distances of 1, 2, and 3 cm measured from the front side (Figure 10). A thermal sensor was placed in the perforated holes while the material was heated from the opposite side using a propane-butane flame at a temperature of 850°C (Figures 11 and 12).

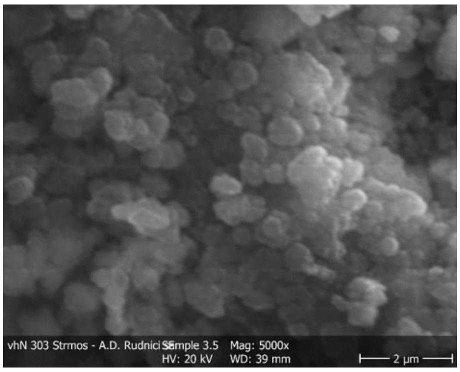

Fig. 9. SEM image of the diatomaceous earth sample

Fig. 10. Perforation of the material at different depths for the placement of the thermal sensor

Fig. 11. Segment of the experimental setup

Fig. 12. Treated sample after the thermal insulation experiment

Table 5

SEM-EDS composition

Components	Mass %
Na_2O	1.31
MgO	1.22
Al_2O_3	14.99
SiO_2	72.17
P_2O_5	0.52
SO_3	0.59
Cl	0.22
K_2O	1.84
CaO	2.55
TiO_2	0.85
MnO	0.11
FeO	3.52

The experiment lasted 60 minutes, and the results for all three measurements are shown in the diagram in Figure 13 and in Table 6.

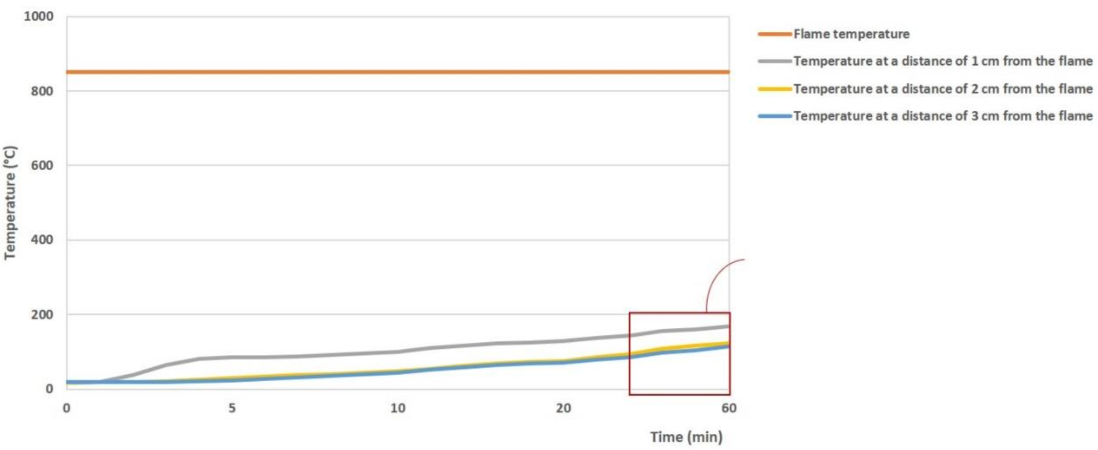

Fig. 13. Diagram of the heat transfer during the thermal treatment

T a b l e 6

Data from the experiment on thermal insulation characteristics

Time (min)	Temperature at a distance of 1 cm from the flame	Temperature at a distance of 2 cm from the flame	Temperature at a distance of 3 cm from the flame
0	18	18.2	19.4
1	19.9	18.4	19.7
2	38.0	19.1	19.6
3	64.0	21.7	20.1
4	82.0	25.7	21.4
5	85.0	29.9	24.0
6	85.0	34.5	27.5
7	88.0	38.0	31.5
8	92.0	41.0	36.1
9	97.0	45.2	39.9
10	101.0	47.3	45.0
12	110.0	55.1	52.3
14	116.5	62.0	59.6
16	122.1	68.1	64.9
18	125.0	73.1	69.9
20	130.0	75.8	72.0
25	136.5	84.8	78.5
30	143.1	93.3	85.3
40	156.0	107.5	99.0
50	160.6	117.0	103.5
60	169.5	124.0	114.9

The results show an exceptionally high thermal insulation property of the compact material, as it maintains a ΔT value higher than 700°C during the 1 hour exposure to the maximum temperature on the other side. This effect of extremely high thermal insulation capability primarily originates from the material's porosity. The distinct separation of curves from the experimental values at 1 cm distance compared to those at 2 and 3 cm results from the following effect: at the first curve, the influence of the porosity of the basic mass dominates, but since the material is sedimentary, with different layers on its contact surface showing varying characteristics during heating, layer separation occurs within the still compact material. These separation segments, as air barriers, further increase the thermal insulation ability. As heat penetrates deeper into the material, the subsequent sediment layers begin to separate due to thermal expansion, with noticeable separation of the curves at 2 and 3 cm, where the next layer starts to open (Figure 14).

The separation of layers during thermal treatment results from the relatively different composition of individual layers, which exhibit different properties as a consequence. For example, the presence of divalent iron in larger or smaller quantities, during its transformation into trivalent iron during the thermal treatment, contributes to the tendency for layer separation. The higher presence of iron in some sediment layers is visually represented by a piece/segment of diatomaceous earth thermally at 800°C, where the higher or lesser presence of iron in different layers is visually noticeable (with varying colour intensity), as clearly shown in Figure 15.

Fig. 14. Profile of the treated compact sample for thermal insulation experiment

Fig. 15. Thermally treated diatomaceous earth sample at 800°C for 2 hours (in an oxidizing atmosphere)

4. CONCLUSIONS

Based on the obtained results from the conducted physico-chemical and mineralogical analyses, as well as previous studies on the diatomaceous earth from Slaviško Pole, the following can be concluded:

The diatomaceous earth from the mentioned locality of Slaviško Pole, predominantly consists of K-feldspar of the microcline type, as well as Na-Ca plagioclases of albite-oligoclase type, along with specific diatom species (silicate spicules of the spongolite type and *Melosira undulata*), interspersed with minor quantities of quartz within a cryptocrystalline matrix.

The chemical composition has been determined across all fractions obtained from the wet sieve analysis, providing insight into the distribution of constituent elements within each fraction. Notably, the highest content of organic matter is determined in the finest fraction (–32 µm), which also exhibits an increased SiO_2 content, as a consequence of higher content of diatoms.

According to the results of the physical-mechanical tests, the compact mass of diatomaceous earth from this locality demonstrates highly favourable properties that align with the requirements of the construction industry. Key attributes include: the feasibility of segmenting elements of relatively large dimensions along sedimentary planes (allowing for processing with minimal energy input); high compressive strength across various orientations (ensuring self-supporting structural integrity); exceptional high thermal insulation capacity (with a temperature gradient of approximately ΔT 700°C over a 1 cm distance within one hour); and resistance to high temperatures without emitting hazardous volatile substances.

The morphology and dimensions of the primary particles/grains (200 – 300 nm), along with their aggregated forms, suggest that this material holds potential as a natural, eco-friendly means of plant protection against specific insect and nematode species. The abrasive action of the diatomaceous earth mechanically affects the exoskeletal joints of insects, while the diatom content induces dehydration in nematodes, thereby reducing their viability.

The combination of open porosity, particle size distribution, absorption and adsorption properties, and chemical stability unequivocally meets the criteria for filtration applications in both potable and waste water treatment. Additionally, this material is well-suited for emergency interventions requiring the removal of hazardous fluids from the environment. Furthermore, when processed into an appropriate granulometric distribution, it can serve as an effective medium for the passive remediation of soils contaminated with heavy metals, leveraging its cation-exchange capacity.

REFERENCES

[1] Wang, Z. Y., Zhang, L. P., Yang, Y. X. (2009): Structural investigation of some important Chinese diatomites, *Glass Physics and Chemistry*, **35** (6), 673–679. DOI: 10.1134/S1087659609060182

[2] Zhang, D. Y, Wang, Y., Cai, J., Pan, J. F., Jiang, X. G., Jiang Y. G. (2012): Bio-manufacturing technology based on diatom micro- and nanostructure, *Chinese Science Bulletin*, **57** (30), 3836–3849. DOI: 10.1007/s11434-012-5410-x

[3] Karaman, E. S., Wang, Z., Di Benedetto, G., Zunino, J. L., Meng, X., Mitra, S. (2019): Fabrication of supercapacitors and flexible electrodes using biosilica from cultured diatoms, *Materials Today Energy*, **11**, 0166–173. DOI: 10.1016/j.mtener.2018.11.004

[4] Hu, Z., Zheng, S., Li, J., Zhang, S., Liu, M., Wang, Z., Li, J., Sun, H. (2022): Pore structure and surface properties of diatomite with mechanical grinding and its influence on humidity control, *Physicochemical Problems of Mineral Processing,* **58** (6), 153509. DOI: 10.37190/ppmp/153509

[5] Li, B., Wang, T., Le, Q., Qin, R., Zhang, Y., Zeng, H. C. (2023): Surface reconstruction, modification and functionalization of natural diatomites for miniaturization of shaped heterogeneous catalysts, *Nano Materials Science*, **5** (3), 293–311. DOI: 10.1016/j.nanoms.2022.05.001

[6] Aggrey, P., Nartey, M., Kan, Y., Cvjetinović, J., Andrews, A., Salimon, A.I., Dragnevski, K.I., Korsunsky, A.M. (2021): On the diatomite-based nanostructure-preserving material synthesis for energy applications, *RSC Advances*, **11** (51), 31884–31922. DOI: 10.1039/d1ra05810j

[7] Villani, M., Onesto, V., Coluccio, M. L., Valpapuram, I., Majewska, R., Alabastri, A., Battista, E., Schirato, A., Calestani, D., Coppedé, N., Zappettini, A., Amato, F., Di Fabrizio, E., Gentile, F., (2019): Transforming diatomaceous earth into sensing devices by surface modification with gold nanoparticles, *Micro and Nano Engineering*, **2**, 29–34. DOI: 10.1016/j.mne.2018.11.006

[8] Wang, C., Li, K., Sun, Q., Zhu, S., Zhang, C., Zhang, Y., Shi, Z., Hu, Y., Zhang, Y. (2023): Diatomite-like $KFeS_2$ for use in high-performance electrodes for energy storage and oxygen evolution, *Nanomaterials*, **13** (4), 643. DOI: 10.3390/nano13040643

[9] De Stefano, M., De Stefano, L. (2005): Nanostructures in diatom frustules: functional morphology of valvocopulae in Cocconeidacean monoraphid taxa, *Journal of Nanoscience and Nanotechnology*, **5** (1), 15–24. DOI: 10.1166/jnn.2005.001

[10] Stanisz, M., Klapiszewski, Ł., Jesionowski, T. (2020): Recent advances in the fabrication and application of biopolymer-based micro- and nanostructures: a comprehensive review, *Chemical Engineering Journal*, **397**, 125409. DOI: 10.1016/j.cej.2020.125409

[11] Arfin, T. (2021): Emerging trends in lab-on-a-chip for biosensing application, *Functionalized Nanomaterials Based Devices for Environmental Applications,* 199–218. DOI: 10.1016/B978-0-12-822245-4.00008-8

[12] Zong, P., Makino, D., Pan, W., Yin, S., Sun, C., Zhang, P., Wan, C., Koumoto, K. (2018): Converting natural diatomite into nanoporous silicon for eco-friendly thermoelectric energy conversion, *Materials & Design*, **154**, 246–253. DOI: 10.1016/j.matdes.2018.05.042

[13] Zeni, V., Baliota, G. V., Benelli, G., Canale, A., Athanassiou, C. G. (2021): Diatomaceous earth for arthropod pest control: back to the future, *Molecules*, **26** (24), 7487. DOI: 10.3390/molecules26247487

[14] Wu, J., Yang, Y. S., Lin, J. (2006): Advanced Tertiary treatment of municipal wastewater using raw and modified diatomite, *Journal of Hazardous Materials*, **127** (1–3), 196–203. DOI: 10.1016/j.jhazmat.2005.07.016

[15] *Mineral commodity summaries 2024*. Reston, Virginia: US Geological Survey, 2024, pp. 68–69.

[16] Reka, A., Pavlovski, B., Fazlija, E., Berisha, A., Pacarizi, M., Daghmehchi, M., Sacalis, C., Jovanovski, G., Makreski, P., Oral, A. (2021): Diatomaceous earth: characterization, thermal modification, and application, *Open Chemistry*, **19** (1), 451–461. DOI: 10.1515/chem-2020-0049

[17] Reka, A., Anovski, T., Bogoevski, S., Pavlovski, B., Boškovski, B. (2014): Physical-chemical and mineralogical-petrograpic examinations of diatomite from deposit near village Roždenr, R. Macedonia, *Geologica Macedonica*, **28** (2), 121–126.

[18] Reka, A., Pavlovski, B., Anovski, T., Bogoevski, S., Boškovski, B. (2015): Phase transformations of amorphous SiO_2 in diatomite at temperature range of 1000–1200°C, *Geologica Macedonica*, **29** (1), 87–92.

[19] Reka, A., Pavlovski, B., Boev, B., Bogoevski, B., Boškovski, B., Lazarova, M., Lamamra, A., Jashari, A., Jovanovski, G., Makreski, P. (2021): Diatomite-evaluation of physico-mechanical, chemical, mineralogical and thermal properties, *Geologica Macedonica*, **35** (1), 5–14. DOI: 10.46763/GEOL21351368005ar

[20] Bogoevski, S., Jančev, S., Boškovski, B. (2014): Characterization of diatomaceous earth from the Slavishko Pole locality in the Republic of Macedonia. *Geologica Macedonica*, **28** (1), 39–43.

[21] Inglethorpe, S. D. J., Pearce, J. M. (1999): *Mineralogy and petrography of diatomite from the Lampang Basin, Changwat Lampang, northern Thailand*. Technical report. British Geological Survey, Nottingham, 1993.

[22] Kützing, F. T. (1844). *Die kieselschaligen Bacillarien oder Diatomeen*. Nordhausen, 152 pp., 30 pls.